DOI: 10.1111/jmcb.12988

STAVROS DEGIANNAKIS
GEORGE FILIS
GRIGORIOS SIOUROUNIS
LORENZO TRAPANI

Superkurtosis

Very little is known on how traditional risk metrics behave under intraday trading. We fill this void by examining the finiteness of the returns' moments and assessing the impact of their infinity in a risk management framework. We show that when intraday trading is considered, assuming finite higher order moments, potential losses are materially larger than what the theory predicts, and they increase exponentially as the trading frequency increases—a phenomenon we call *superkurtosis*. Hence, the use of the current risk management techniques under intraday trading imposes threats to the stability of financial markets, as capital ratios are severely underestimated.

JEL codes: C12, C54, F30, G10, G15, G17
Keywords: finite moments, risk management, superkurtosis, ultra-high frequency trading

HIGHLY SOPHISTICATED ALGORITHMS AND FAST computer technology have originated a new class of trading known as "intraday trading." Intraday trading has numerous advantages: it offers a great deal of liquidity in the market; it facilitates the instantaneous transmission of information into prices, pushing markets to be more efficient; and it creates a market place for small (retail) as well as large investors (institutions).

However, intraday trading also presents unique challenges (see, e.g., the Final Project Report from The Government Office for Science, London - 2012). Chiefly, it has been criticized as liable to cause large market crashes that may be amplified by the

STAVROS DEGIANNAKIS *is a Professor of Econometrics and Statistics, Department of Economic and Regional Development, Panteion University of Social and Political Science, & Research and Economic Analysis Department, Bank of Greece* (*E-mail*: sdegiannakis@panteion.gr). GEORGE FILIS *is an Assistant Professor of Economics, Department of Economics, University of Patras* (*E-mail*: gfilis@upatras.gr). GRIGORIOS SIOUROUNIS *is an Assistant Professor of Economics, Department of Economic and Regional Development, Panteion University of Social and Political Science, & Department of Economics, Brown University* (*E-mail*: grigorios_siourounis@brown.edu). LORENZO TRAPANI *is a Professor of Econometrics, School of Economics, University of Nottingham* (*E-mail*: lorenzo.trapani@nottingham.ac.uk).

Received March 25, 2020; and accepted in revised form March 28, 2022.

influx of algorithmic trading and the order clustering caused by unintended trading strategy coordination (see, e.g., Beddington et al. 2012; Kirilenko et al. 2017; Manhire 2018; and media coverage such as Brush, Schoenberg, and Ring 2015). Hence, regulators (see the Press Release, European Parliament, MEPs Vote Laws to Regulate Financial Markets and Curb High Frequency Trading (April 15, 2014)), economists (e.g., Kirilenko and Lo 2013), and law scholars (e.g., Yadav 2015) have proposed measures to mitigate such trading behavior.

As a consequence of the issues discussed above, market participants are required to measure and report several market risk metrics, and to take them into account when calculating their regulated capital requirements. For example, on January 16th, 2016, the Basel Committee on Banking Supervision (henceforth, "the Committee") published a document that revised standards for minimum capital requirements for Market Risk. In addition, the Committee had also produced three consultative papers on the Fundamental review of the trading book, namely (i) fundamental review of the trading book, May 2012, (ii) a revised market risk framework, October 2013, and (iii) fundamental review of the trading book: Outstanding issues, December 2014. Furthermore, ECB imposes capital requirements (via the Capital Requirements Regulation) on institutions who engage in intraday trading. Such requirements are based on risk metrics or asset volatility. [1] However, standards set by regulators are based on risk metrics that are calculated—at most—at daily frequency. Given that intraday trading takes place at higher frequencies, this leaves the market risk, generated by such trading activity, largely as a dark pool. Indeed, very little is known about market risk associated with intraday trading; similarly, only little analysis has been conducted on how traditional risk metrics such as value-at-risk (*VaR*, hereafter) or Expected Shortfall (*ES*, hereafter) behave at such high-frequency trading. The investigation of this issue is arguably of immense importance, due to the fact that typical risk metrics users assume that high-order moments of asset returns at intraday frequency are finite. This assumption is based on the fact that such moments are finite at lower, for example, daily, frequency, which may be not hold true for higher frequencies. Consequently, the *VaR* and *ES* are calculated under the assumptions that high-order moments are finite, typically using the quantiles of the normal distribution. In turn, such risk metrics computations are assumed to adequately capture capital requirements, which may be grossly incorrect in the presence of heavy tails. Of course, it is perfectly possible to compute the *VaR* and *ES* without assuming normality. However, existing methodologies require several assumptions that may not be satisfied: for example, extreme-value-theory-based methodologies usually require the *i.i.d.* assumption (see Manganelli and Engle 2001), which is highly unlikely to be satisfied by intraday returns. Thus, prior to calculating any risk metric, it is of vital importance to have a deep understanding of the properties of the data. Despite its importance,

1. For details, see https://www.bankingsupervision.europa.eu/press/publications/newsletter/2019/html/ssm.nl190213-5.en.html

the assumption of finite moments has not been formally tested thus far to the best of our knowledge.

In this study, we fill the gaps discussed above by offering two contributions. First, we develop a methodology to check whether high-order moments are finite. We point out that, in this context, very few tests are available. One exception is Trapani (2016), but his test (as we discuss in more detail below) produces nonreplicable results, so that different researchers using the same data sets may obtain different results as to the finiteness, or not, of high-order moments. Conversely, our methodology overcomes this issue, ensuring that all researchers using the same data set will obtain the same results and draw the same conclusions. As a second contribution, we assess the impact of having infinite moments in a risk management framework. In our empirical analysis, we focus on the foreign exchange market, which is justified by the fact that—in that context—trading has become increasingly electronic and automated. The use of intraday frequency algorithms and machine learning protocols are continuously increasing in the foreign exchange market with more than 65% of the more than 5 trillion dollars daily volume to be traded from such algorithms. In addition, more than 80% of Central Banks monitor Fasted Paced Electronic Markets operations and 60% is for market stability reasons alone.

In our empirical analysis (Section 2), we apply our test to check whether the first four moments are finite, using intraday data from the currency markets. We find that the distribution of the returns of the assets traded intraday does not have finite absolute moments of order higher than 3,[2] implying that mainly the kurtosis is infinite at intraday frequencies. In contrast, daily data do have finite moments. The finiteness of high-order moments at lower frequencies may explain why the traditional, Gaussian-based way of computing VaR and ES is also used at high frequency. However, using a distribution that admits all moments in the presence of heavy tails may lead to wrong conclusions: in Section 2.3, we illustrate the consequences of neglecting this feature, calculating the high losses incurred by (and the short survival of) an investor who ignores this issue. To shed further light, in Section 3, we report extensive Monte Carlo evidence, showing that VaR and ES are much larger than implied, for example, by the classical risk management approaches. We find that this is due to two reasons. First, the natural increase in the sample size as the frequency increases directly affects potential losses. Second, we find clear numerical evidence that, at higher frequencies, data sampled from a distribution that has heavy tails tend to have higher sample moments (chiefly, higher kurtosis) than the theory would predict.[3] In turn, this affects the potential losses associated with VaR or ES. To confirm this striking empirical

2. We note that there are intraday frequencies that exhibit infinite third moment. However, our analysis is focused on the severe implications brought about by the fourth moment being infinite in intraday frequencies, since our testing and simulations show that even when the third moment is infinite, this does not alter the VaR or ES metrics in any statistically significant manner.

3. This consideration is based on the Marcinkiewicz–Zygmund strong law of large numbers (SLLNs), which provides an upper bound on the growth rate of sample moments when the corresponding population moments are infinite.

finding, and to disentangle possible sources of the extreme (infinite) potential losses, we carry out an extensive series of simulations. Evidence from simulated data suggests that, on the one hand, the estimated kurtosis grows as the sampling frequency increases (as the SLLN implies); yet, on the other hand, the growth pattern exhibits a much faster rate than the one implied by the SLLN bound. Thus, kurtosis diverges much faster from its theoretical path as the sampling frequency increases, contributing significantly to the increase of the potential losses at intraday trading. Hence, the simulated data lend strong support to our empirical conclusions generated from the use of actual currency pairs data. We call this phenomenon *superkurtosis*; it implies that traditional risk metrics are not a good measure for the true market risk (see also Bradley and Taqqu 2003), and should therefore not be employed to gauge capital adequacy under intraday trading.

The remainder of the paper is organized as follows. Section 1 describes the methods used for the test of moments, as well as, for the assessment of the impact of these moments on risk management. Section 2 presents our empirical results from the real data and Section 3 for the simulated data. Finally, Section 4 concludes the study and provides ideas for future research. Technical results and further tables are in the Appendix.

1. METHODOLOGY

Our methodology consists of two steps. We start by verifying whether higher order moments are finite (Section 1.1); we then turn to assessing the impact of having infinite high-order moments on risk metrics (Section 1.2).

1.1 Testing for the Finiteness of the Asset Returns' Moments

In this section, we discuss testing for the finiteness of the moments of a random variable X, given a sample $\{x_t\}_{t=1}^{T}$, also proposing an improved, replicable version of the original test by Trapani (2016)—see below for details. Our hypothesis testing framework is as follows:

$$\begin{cases} H_0 : E|X|^k = \infty \\ H_A : E|X|^k < \infty \end{cases}, \tag{1}$$

with $k = 2$, 3 and 4. In (1), the null hypothesis is the *infinity* of the k^{th} absolute moment. As in Trapani (2016), for each k, test statistics are based on

$$\mu_k = c_k \times \frac{T^{-1}\sum_{t=1}^{T}|x_t|^k}{\left(T^{-1}\sum_{t=1}^{T}|x_t|^p\right)^{k/p}}, \tag{2}$$

where $p = \min\{k-1, 2\}$ and c_k is defined in equation (A.3) in Appendix A. Hence, we construct the statistic

$$\psi_k = \exp(\mu_k) - 1. \tag{3}$$

Trapani (2016) showed that ψ_k diverges to positive infinity under H_0, whereas it drifts to zero under H_A. To produce a test statistic that has a well-defined limiting law, ψ_k is randomized by using the following algorithm.

Step 1 Randomly generate an *i.i.d.* $N(0,1)$ sample of size $R = \lfloor T^{1/2} \rfloor$, say $\{\xi_j^{(k)}\}_{j=1}^R$, independently across k, and define $\{\psi_k^{1/2} \times \xi_j^{(k)}\}_{j=1}^R$.
Step 2 For $u \in \{-\sqrt{2}, \sqrt{2}\}$, generate $\zeta_{j,T}^{(k)}(u) = I(\psi_k^{1/2} \times \xi_j^{(k)} \leq u)$, $1 \leq j \leq r$.
Step 3 For each u, define

$$\vartheta_{T,R}^{(k)}(u) = \frac{2}{\sqrt{R}} \sum_{j=1}^{R} \left[\zeta_{j,T}^{(k)}(u) - \frac{1}{2} \right], \tag{4}$$

and finally, the test statistic

$$\Theta_{T,R}^{(k)} = \frac{1}{2} \left[\left(\vartheta_{T,R}^{(k)}\left(-\sqrt{2}\right) \right)^2 + \left(\vartheta_{T,R}^{(k)}\left(\sqrt{2}\right) \right)^2 \right]. \tag{5}$$

The limiting distribution of $\Theta_{T,R}^{(k)}$ is in Theorem 1 in Appendix A; in essence, under the null, $\Theta_{T,R}^{(k)}$ follows a chi-squared distribution with one degree of freedom (henceforth χ_1^2). However, this result is different from a standard limit theorem, and it suffers from a replicability issue which we now proceed to explain. Indeed, under H_0, it holds that

$$\lim_{\min(T,R)\to\infty} P^*\{\Theta_{T,R}^{(k)} \geq c_\alpha\} = \alpha, \tag{6}$$

conditional on the sample, where c_α is a critical value defined by $P(\chi_1^2 \geq c_\alpha) = \alpha$. However, the test statistic $\Theta_{T,R}^{(k)}$ is constructed using the randomness $\{\xi_j^{(k)}\}_{j=1}^R$, which does not vanish asymptotically. As a consequence, different researchers using the same data will obtain different values of $\Theta_{T,R}^{(k)}$, and therefore, different p-values; indeed, if an infinite number of researchers were to carry out the test, the p-values would follow a uniform distribution on [0, 1]. This is a well-known feature of randomized tests (see, e.g., the discussion in Horváth and Trapani 2019).

To address the issue mentioned above, we construct a "strong" (i.e., valid almost surely) decision rule that ensures that the decision between H_0 and H_A is not subject to such arbitrariness, and that all researchers will end up having the same outcome. Our decision rule works as follows. Each researcher, instead of computing $\Theta_{T,R}^{(k)}$ just once,

will compute the test statistic S times, at each time s using an independent sequence $\{\xi_j^{(s)}, 1 \leq j \leq R\}$ for $1 \leq s \leq S$, thence defining

$$Q^{(k)}(\alpha) = S^{-1} \sum_{s=1}^{S} I\Big[\Theta_{T,R,s}^{(k)} \leq c_\alpha\Big], \tag{7}$$

where $\Theta_{T,R,s}^{(k)}$ is the test statistic computed according to the algorithm above using the artificial sample $\{\xi_j^{(s)}, 1 \leq j \leq R\}$. The function $Q^{(k)}(\alpha)$ is related to the "fuzzy confidence interval" discussed in equation (1.1b) in Geyer and Meeden (2005). We note (heuristically) that an immediate consequence of Theorem 1 is

$$\begin{aligned} &\lim_{\min(T,R,S)\to\infty} P^*\{Q^{(k)}(\alpha) = 1-\alpha\} = 1 \text{ under } H_0 \\ &\lim_{\min(T,R,S)\to\infty} P^*\{Q^{(k)}(\alpha) = 0\} = 1 \text{ under } H_A. \end{aligned} \tag{8}$$

This indicates that, as $S \to \infty$, $Q^{(k)}(\alpha)$ has been "derandomized" — that is, the randomness added by the researcher has been washed out, and the conclusions drawn from a test based on $Q^{(k)}(\alpha)$ are exactly the same across all researchers. We formalize the properties of $Q^{(k)}(\alpha)$ in Theorem 2 in Appendix A. Based on the results in Theorem 2, a decision rule in favor of H_0 can be based on

$$Q^{(k)}(\alpha) \geq (1-\alpha) - \frac{\sqrt{\alpha(1-\alpha)}}{f(S)}, \tag{9}$$

for all sequences $f(S) \to \infty$ such that $f(S) = o(S^{1/2})$. In the empirics section, we discuss the choice of $f(S)$ and the robustness of $Q^{(k)}(\alpha)$ to its choice.

1.2 Assessing the Impact of Infinite Moments in Risk Management

We consider a representative trader with unlimited capital, who wants to calculate her *VaR* measure at each point in time. Without loss of generality, each trading day t is divided in τ equidistant intraday subintervals. The observed prices at day t are denoted as P_{t_j}, for $j = 1, 2, \ldots, \tau$, with sample frequency defined as $m = \tau^{-1}$. We define daily log-returns as $y_t = \log P_{t_\tau} - \log P_{(t-1)_\tau}$, and intraday log-returns as $y_{t_j} = \log P_{t_j} - \log P_{t_{j-1}}$.

The *VaR* for a long trading position at $(1-p)$ level of confidence, at sampling (trading) frequency m, is denoted as $VaR_{(1-p)}^{(m)}$, defined such that $P(y_{t_j} \leq VaR_{(1-p)}^{(m)}) = p$. The $VaR_{(1-p)}^{(m)}$ is computed nonparametrically as the p-quantile of the intraday log-returns at sampling frequency m: $VaR_{(1-p)}^{(m)} = f_p(\{y_{t_j}\}_{j=1,\ldots,\tau}^{t=1,\ldots,T})$.[4] We measure the

4. The *VaR* of intraday log-returns y_{t_j} for a short trading position at $(1-p)$ level of confidence at sampling frequency m is $P(y_{t_j} \geq VaR_{(1-p)}^{(m)}) = (1-p)$.

potential losses conditional to a *VaR* violation (i.e., the losses that occur when the returns are lower than the *VaR* measure) by constructing an evaluation function, $l_{t_j}^{(m)}$ that measures the absolute distance between actual returns, y_{t_j}, and the *VaR* measure, that is, the potential loss ($l_{t_j}^{(m)}$):

$$l_{t_j}^{(m)} = \begin{cases} |y_{t_j} - VaR_{(1-p)}^{(m)}| & \text{if } y_{t_j} < VaR_{(1-p)}^{(m)} \\ 0 & \text{otherwise.} \end{cases} . \tag{10}$$

We note that the expected shortfall, recently proposed as an alternative risk measure, is the expectation of the potential loss ($\mathbb{E}(l_{t_j}^{(m)})$), given that the *VaR* violation is present.

The total potential losses over the sample period are computed as $L^{(m)} = \sum_{t=1}^{T} \sum_{j=1}^{\tau} l_{t_j}^{(m)}$. To allow comparison across the different sampling frequencies, we also compute the daily adjusted losses per *VaR* violation as $\bar{L}^{(m)} = 1361(Nm)^{-1}L^{(m)}$, for $N = \sum_{t=1}^{T} \sum_{j=1}^{\tau} I_{t_j}^{(m)}$, where:

$$I_{t_j}^{(m)} = \begin{cases} 1 & \text{if } y_{t_j} < VaR_{(1-p)}^{(m)} \\ 0 & \text{otherwise.} \end{cases} \tag{11}$$

We multiply the number of violations by the daily adjustment, $1,361/m$, where 1,361 reflects the 1-minute observations per day that the market is open.

2. EMPIRICAL FINDINGS FROM ACTUAL DATA OF THREE CURRENCY PAIRS

In this section, we carry out an empirical exercise, where we *(i)* check whether our data have heavy tails or not (by testing for the finiteness of up to the fourth moment); and *(ii)* evaluate the potential losses when using a strategy that fails to acknowledge that higher order moments are infinite. We find that, when considering intraday frequency data, higher order moments such as the kurtosis are infinite; and that potential losses tend, in such cases, to be much higher than anticipated.

2.1 Data Description

We use 1-minute data of the front-month futures contracts, as well as, the spot prices, for the EUR/USD, GBP/USD, and CAD/USD exchange rates, obtained from TickData and HistData, respectively. The period of the study spans from January 3, 2000 to August 5, 2015 for the futures data, whereas, due to data availability issues, the sample period for the spot prices runs from January 3, 2005 to August 5, 2015. We focus on a sample of the G10 exchange rate market as it is considered the deepest continuously trading market in the world, so that we do not have to take into consideration significant data alterations. The choice of the specific currency pairs is justified by the fact that *(i)* they are among the most liquid, and *(ii)* they represent the most

heavily traded exchange rate for financial transactions. Our sample consists of 3,990 trading days, which contain more than 25 million 1-minute data in total.

Descriptive statistics—for the currency pairs' spot and futures returns for sampling (trading) frequencies from 1 minute to 1 day—are summarized in Table B.1 in Appendix B. We note that volatility is falling linearly as the sampling frequency is increasing. By contrast, the third moment (skewness) does not change materially from symmetry at the different frequencies. More importantly, the fourth moment (kurtosis) shows the well-documented leptokurtosis, which increases dramatically as the sampling frequency increases. This is particularly evident for the futures price returns, which suggests that investors in the futures market are exposed to greater tail risk. Of course, the magnitude of kurtosis at the higher frequencies differs among the different crosses, with the higher values to be observed in the EUR/USD.

2.2 Testing for the Finiteness of Higher Order Moments

We start our analysis with the results on the finiteness of moments in Tables 1 and 2.[5] When computing (9), we used the same specifications as in the paper by Trapani (2016)—namely, we set $R = \lfloor T^{1/2} \rfloor$ (note that T is a much larger number than in the simulations considered in Trapani (2016), so R is likely to be much larger than needed). Consistently with Theorem 2, we chose $S = 2,000$, which is essentially the same order of magnitude as R for all cases considered; we would like to point out that we tried to vary S, but results are virtually unchanged. Finally, in the computation of the threshold for $Q^{(k)}(\alpha)$, we use $f(S) = S^{1/4}$; we note that functions like $f(S) = S^a$, for $0 < a < \frac{1}{2}$, are in principle all acceptable. We experimented with different functional forms for $f(S)$, using, for example, $f(S) = S^{1/3}$ and $f(S) = S^{1/5}$, but results are exactly the same, which illustrates the robustness of our procedure to this specification.

The results in Tables 1 and 2 show that the second moment is finite across all currencies and sampling frequencies (for both spot and futures returns), whereas skewness seems to exist in most cases, with the main exceptions being the 1–20 m frequencies for the EUR/USD and GBP/USD futures. More importantly, though, for all intraday sampling frequencies across the three currency pairs (either in their futures or spot returns), the null hypotheses of infinite fourth moment cannot be rejected, lending preliminary support to the *superkurtosis* phenomenon. On the other hand, moving to lower sampling frequencies, that is, daily, we find evidence that all moments are finite.

2.3 The Impact of the Infinity of Moments in Intraday Returns

The results presented in Tables 1 and 2 seem to suggest that risk management tools, such as the *VaR* or *ES*, that are used by implicitly assuming finite moments, might

5. We have also considered lower frequencies than the daily (e.g., weekly, biweekly, and so on) and the results show that all moments continue to be finite. These unreported results are available from the authors upon request.

TABLE 1

TESTS FOR THE FINITENESS OF MOMENTS FOR THE FUTURES CURRENCY PAIRS AT DIFFERENT SAMPLING (TRADING) FREQUENCIES

Frequency	Size	*St.Dev.*		*Skewness*		*Kurtosis*	
		EUR/USD futures					
		St. Dev.	$Q^{(2)}(\alpha)$	*Skewness*	$Q^{(3)}(\alpha)$	*Kurtosis*	$Q^{(4)}(\alpha)$
1m	5,350,727	1.88×10^{-4}	0.000	1.806	0.948*	729.97	0.938*
2m	2,675,321	2.63×10^{-4}	0.000	1.396	0.948*	395.10	0.941*
5m	1,070,147	4.07×10^{-4}	0.000	0.799	0.953*	161.38	0.957*
10m	535,031	5.69×10^{-4}	0.000	0.545	0.938*	85.43	0.939
15m	356,717	6.92×10^{-4}	0.000	0.439	0.946*	62.34	0.942*
20m	269,462	7.94×10^{-4}	0.000	0.469	0.937*	52.64	0.941*
30m	178,316	9.70×10^{-4}	0.000	0.304	0.902	36.85	0.948*
60m	95,138	13.28×10^{-4}	0.000	0.271	0.820	24.67	0.937*
daily	3,990	64.48×10^{-4}	0.000	0.033	0.000	4.33	0.000
		GBP/USD futures					
		St. Dev.	$Q^{(2)}(\alpha)$	*Skewness*	$Q^{(3)}(\alpha)$	*Kurtosis*	$Q^{(4)}(\alpha)$
1m	5,142,433	1.78×10^{-4}	0.000	−0.487	0.948*	269.39	0.947*
2m	2,571,564	2.12×10^{-4}	0.000	−0.500	0.945*	119.22	0.940*
5m	1,029,113	3.16×10^{-4}	0.000	−0.422	0.958*	85.45	0.944*
10m	514,904	4.42×10^{-4}	0.000	−0.364	0.926*	61.41	0.944*
15m	343,557	5.29×10^{-4}	0.000	−0.348	0.905	36.53	0.942*
20m	257,800	6.16×10^{-4}	0.000	−0.345	0.929*	41.92	0.940*
30m	172,128	7.44×10^{-4}	0.000	−0.317	0.878	27.83	0.946*
60m	89,664	10.14×10^{-4}	0.000	−0.288	0.729	19.71	0.947*
daily	3,990	56.79×10^{-4}	0.000	−0.321	0.000	5.33	0.000
		CAD/USD futures					
		St. Dev.	$Q^{(2)}(\alpha)$	*Skewness*	$Q^{(3)}(\alpha)$	*Kurtosis*	$Q^{(4)}(\alpha)$
1m	5,142,433	1.87×10^{-4}	0.000	0.116	0.942*	103.30	0.947*
2m	2,571,564	2.57×10^{-4}	0.000	0.067	0.927*	64.32	0.939*
5m	1,029,114	3.96×10^{-4}	0.000	0.029	0.903	39.46	0.945*
10m	514,904	5.51×10^{-4}	0.000	0.049	0.860	29.89	0.944*
15m	343,561	6.64×10^{-4}	0.000	−0.035	0.801	24.33	0.952*
20m	257,800	7.63×10^{-4}	0.000	0.067	0.786	22.01	0.951*
30m	172,128	9.24×10^{-4}	0.000	0.021	0.717	19.25	0.940*
60m	89,664	12.31×10^{-4}	0.000	0.192	0.686	17.48	0.945*
daily	3,990	58.10×10^{-4}	0.000	−0.142	0.000	6.01	0.000

[5]NOTE: For each currency, we report the value of the relevant descriptive statistic, and the value of the function $Q^{(k)}(\alpha)$ as defined in equation (7). The asterisks next to each value of $Q^{(k)}(\alpha)$ indicate that $Q^{(k)}(\alpha)$ exceeds the threshold defined in (9). In turn, this entails that the null that the corresponding, kth absolute moment is infinite is *not rejected* at nominal level α, thus indicating that the relevant moment is infinite.

be inappropriate to assess the true underlining risk of loss in the ultrahigh frequencies. To ascertain this, we consider a scenario where traders assume that high-order moments are finite at the intraday frequencies. Under this scenario, we calculate the potential losses ($L^{(m)}$ and $\bar{L}^{(m)}$), conditional to *VaR* violation, as shown in Section 1.2 (see Figures 1 and 2, which depict the results for the futures and spot price returns, respectively).

In all cases considered in Figure 1, potential losses are decidedly higher for the higher sampling (trading) frequencies, while they decrease rapidly as the sampling (trading) frequency decreases. This holds for both the total potential losses ($L^{(m)}$) and the daily adjusted potential losses ($\bar{L}^{(m)}$). For instance, in the 1-minute trading

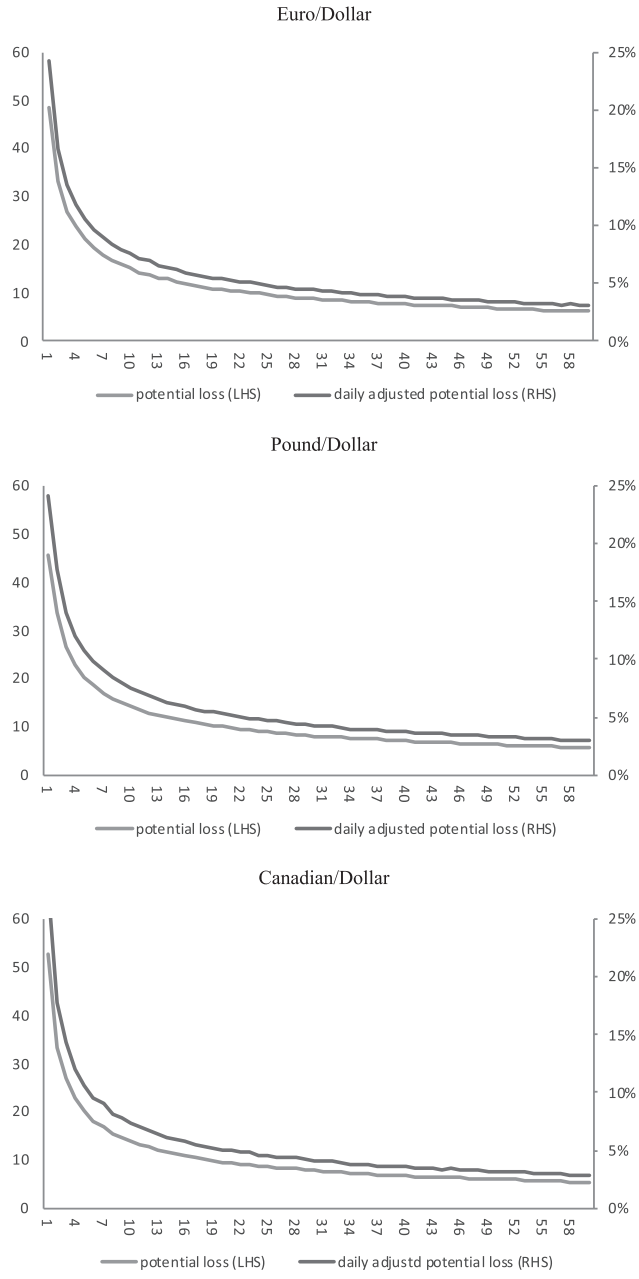

Fig 1. Trader's Potential Capital Losses, on the Three Futures Exchange Rates, above the Anticipated Losses from the *VaR* Measure.

NOTES: The *x*-axis denotes the $m = 1,...,60$ minute intraday sampling (trading) frequencies. The values in the *y*-axis refer to number of times, whereas in the *z*-axis refers to percentages.

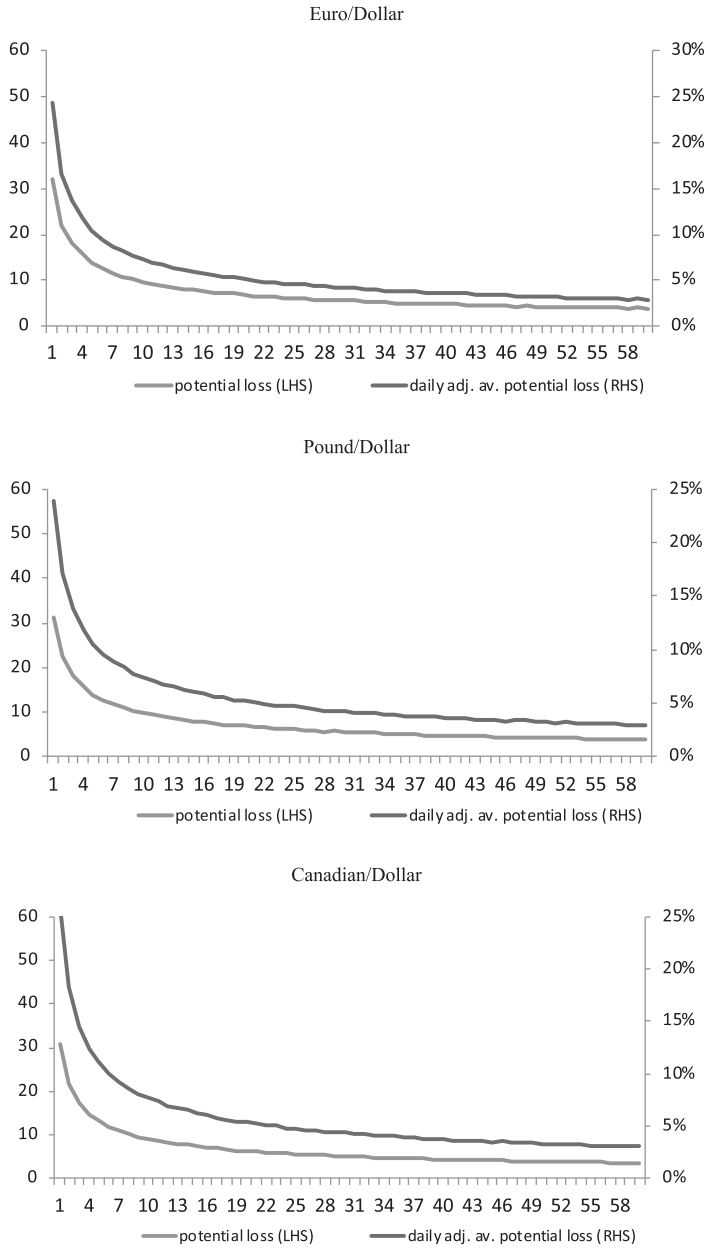

Fig 2. Trader's Potential Capital Losses, on the Three Spot Exchange Rates, above the Anticipated Losses from the *VaR* Measure.

NOTES: The *x*-axis denotes the $m = 1,...,60$ minute intraday sampling (trading) frequencies. The values in the *y*-axis refer to number of times, whereas in the *z*-axis refers to percentages.

TABLE 2

TESTS THE FINITENESS OF MOMENTS FOR THE SPOT CURRENCY PAIRS AT DIFFERENT SAMPLING (TRADING) FREQUENCIES

Frequency	Size	*St.Dev.*		*Skewness*		*Kurtosis*	
			EUR/USD spot				
		St. Dev.	$Q^{(2)}(\alpha)$	*Skewness*	$Q^{(3)}(\alpha)$	*Kurtosis*	$Q^{(4)}(\alpha)$
1m	3,814,542	1.80×10^{-4}	0.000	0.337	0.917*	79.58	0.941*
2m	1,907,174	2.55×10^{-4}	0.000	0.117	0.920*	71.02	0.941*
5m	762,817	3.97×10^{-4}	0.000	0.155	0.880	45.01	0.953*
10m	381,417	5.55×10^{-4}	0.000	0.071	0.738	26.34	0.953*
15m	254,275	6.78×10^{-4}	0.000	0.353	0.818	30.59	0.941*
20m	190,704	7.78×10^{-4}	0.000	−0.001	0.622	20.03	0.953*
30m	127,134	9.51×10^{-4}	0.000	0.173	0.619	20.65	0.946*
60m	63,564	13.35×10^{-4}	0.000	0.047	0.350	13.93	0.935*
daily	2,662	63.12×10^{-4}	0.000	0.198	0.002	6.55	0.004
			GBP/USD spot				
		St. Dev.	$Q^{(2)}(\alpha)$	*Skewness*	$Q^{(3)}(\alpha)$	*Kurtosis*	$Q^{(4)}(\alpha)$
1m	3,791,546	1.74×10^{-4}	0.000	−0.025	0.892	46.44	0.941*
2m	1,895,673	2.47×10^{-4}	0.000	−0.088	0.913	48.42	0.945*
5m	758,224	3.86×10^{-4}	0.000	−0.096	0.868	32.66	0.944*
10m	379,114	5.41×10^{-4}	0.000	−0.107	0.781	25.23	0.951*
15m	252,740	6.55×10^{-4}	0.000	−0.075	0.707	21.23	0.949*
20m	189,553	7.57×10^{-4}	0.000	−0.129	0.776	24.21	0.955*
30m	126,366	9.18×10^{-4}	0.000	−0.056	0.601	17.84	0.942*
60m	63,180	12.91×10^{-4}	0.000	−0.113	0.524	16.15	0.940*
daily	2,666	60.99×10^{-4}	0.000	0.357	0.000	8.12	0.205
			CAD/USD spot				
		St. Dev.	$Q^{(2)}(\alpha)$	*Skewness*	$Q^{(3)}(\alpha)$	*Kurtosis*	$Q^{(4)}(\alpha)$
1m	3,416,089	1.97×10^{-4}	0.000	0.049	0.856	40.32	0.950*
2m	1,707,811	2.77×10^{-4}	0.000	−0.045	0.855	40.25	0.954*
5m	683,011	4.32×10^{-4}	0.000	−0.033	0.699	24.17	0.948*
10m	341,507	6.00×10^{-4}	0.000	−0.079	0.562	19.89	0.944*
15m	227,669	7.34×10^{-4}	0.000	−0.002	0.533	18.88	0.948*
20m	170,749	8.41×10^{-4}	0.000	−0.038	0.454	16.45	0.946*
30m	113,829	10.26×10^{-4}	0.000	0.067	0.400	15.13	0.935*
60m	56,911	14.35×10^{-4}	0.000	0.044	0.337	14.50	0.934*
daily	2,686	65.76×10^{-4}	0.000	0.002	0.000	6.40	0.003

[5] NOTE: The numbers in the table have the same meaning as in Table 1.

frequency of the EUR/USD futures prices, we observe that a trader would have lost 48 times more capital than anticipated by the *VaR*, whereas the daily adjusted losses, for the same frequency, are about 25% more. Similar figures are reported for the GBP/USD and CAD/USD futures prices as well.[6]

We supplement our analysis by focusing also on the spot prices of the three currency pairs. We do so, since the spot and futures prices are related via covered interest rate parity, and thus, the empirical findings could be driven by the interest

6. Please note that we have also considered a short position in the currency pairs and the results are qualitatively similar, suggesting that the infinity of the third moment that was exhibited in some frequencies cannot be blamed for the observed behavior of the potential losses.

rate differential component. Figure 2 depicts the potential losses and daily adjusted potential losses conditional to *VaR* violations, using the spot exchange rates. We observe that the potential losses increase exponentially as the trading frequency increases. For instance, the potential losses in all currencies are 30 times larger at the 1-minute sampling frequency, suggesting that a trader is anticipated to lose 30 times more capital (or about 25% based on the daily adjusted losses) more than anticipated by the *VaR*, when she trades on a 1-minute frequency. Although the magnitude of the potential losses is lower compared to the futures prices (for the Euro/Dollar futures, the potential losses were 48 times higher at the 1-minute sampling frequency), we can immediately understand that the main findings observed using the futures prices remain unchanged for the case of spot prices.

To elaborate further on our key finding, we proceed with a simple example of the consequence of ignoring the infinity of high-order moments and, in particular, the *superkurtosis* phenomenon, by quantifying how much a trader is miscalculating her expected losses. To do so, we assume three representative traders that each have an initial capital of \$10, 000. The only difference among the three traders is the choice of trading frequency. Indicatively, we assume that the first trader chooses to trade every minute, the second every 60 minutes and the third trader makes her trades on a daily basis. Furthermore, the traders have an investment horizon equal to our sample period. Each trader calculates her 95% *VaR* measure and invests the capital that respects the *VaR* in the foreign exchange market at each point in time. To quantify the miscalculation of the potential losses, we proceed as follows. When the trader makes a positive return or a loss that falls within the *VaR*, then we report this as a zero potential excess loss. However, when the trader suffers a loss greater than the 95% *VaR* number, then we calculate the excess loss beyond and above the *VaR* (for the specific minute, hour or day). We do that for all trading observations of each trader and we then aggregate these excess losses over the sample period. We do so to quantify the maximum potential excess losses (rather than the actual losses) of each trader. For brevity, Figure 3 presents only the cumulative potential excess losses for each trader for the EUR/USD futures market.

Figure 3 clearly demonstrates the severity of the issue discussed in this paper. The potential excess losses for 1 minute trader is massively higher compared to the daily trader. In particular, based on the study period used in this paper, the potential excess loss for the 1 minute trader reaches the level of almost \$600, 000, which means that the trader can potentially deplete her capital within a very short period of time (in the first 3-months in our numerical example), showing that *VaR* is heavily misleading. By contrast, for the daily trader, this amount is about \$9, 000, which means that this trader never depletes her capital and thus *VaR* is a valid risk management metric in this context.

2.4 Robustness Analysis

To complement our empirical analysis based on the actual intraday data of the three chosen currency pairs, we further assess our findings by distinguishing between

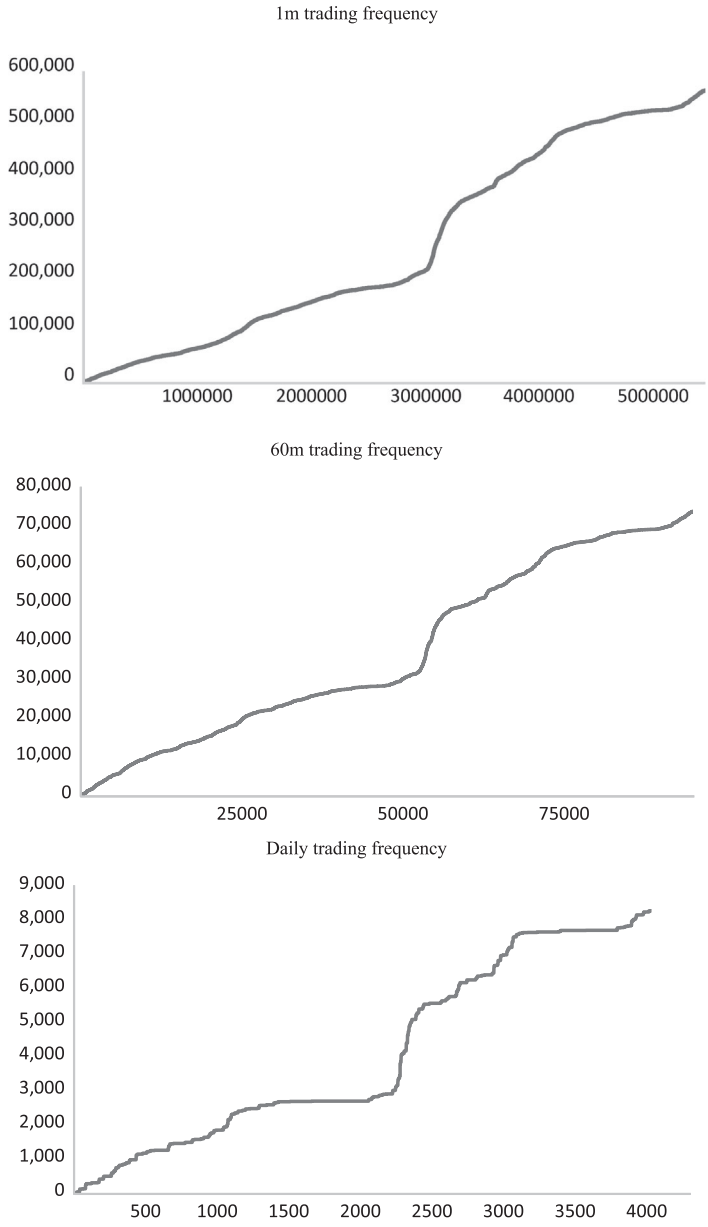

Fig 3. Traders' Potential Capital Losses in $ Terms, on the EUR/USD Futures Exchange Rate, above the Anticipated Losses from the 95% *VaR*.

NOTES: The figure shows the potential losses that can be suffered from three representative traders of the EUR/USD futures prices. From the top panel to the bottom, we show the cumulative potential losses for the 1 minute trader, the 60 minute trader, and the daily trader. The *y*-axis denotes the amount of potential excess losses in $. The values in the *x*-axes refer to number observations, over the sample period, for the 1 minute trader, 60 minutes trader, and the daily trader.

intraday and overnight returns, as well as, between the ebb and flow trading periods. Finally, we assess the validity of our findings using a carry trade strategy where the investor goes long on the high interest rate and short on the low interest rate currency.

Initially, we remove the overnight returns from the intraday returns of our futures prices. We time stamp our analysis considering as closing times the period between 4:00 p.m. and 5:00 p.m. Chicago time. Thus, we remove the overnight returns (which are defined as the returns occurring between the closing time of the day and the opening time of the next day) and we reestimate the potential losses and daily adjusted potential losses. Figure 4 presents our results.

Similarly to our previous analysis, we note that removing the overnight returns does not alter our main findings, showing that our results are not driven by the potential price jumps that could be observed when the market is considered closed.

Next, we proceed with an additional robustness check, distinguishing the futures price returns between the ebb and flow transaction periods. The busiest time zones for foreign exchange trading are London and New York. Thus, we isolate the intraday futures returns of our currency pairs for the time period 2:00 a.m. to 3:00 p.m. Chicago time, which denote the high trading period and we leave the remaining opening hours as the low trading period. The results are shown in Figures 5 and 6. The results are qualitatively similar to our initial findings from Figure 1.

To complement further our empirical analysis based on actual intraday data, we proceed with a currency carry trade. To do so, we use one of the most popular carry trades, which is going long the Australian Dollar (AUD) and short the Japanese Yen (JPY). As in the previous analysis, Figure 7 suggests that the main findings not only still persist, but they are exacerbated. Using once again the 1-minute sampling frequency, we document that the potential losses are more than 60 times higher compared to the amount anticipated by the *VaR*, which translates into 45% more daily adjusted potential losses.

3. FINDINGS FROM SIMULATED DATA

Our analysis above shows that the *superkurtosis* phenomenon, that is, the infinite kurtosis, could be the source of the extreme potential losses as the sampling (trading) frequency increases. However, the actual source of these losses is rather unclear. Thus, to shed light in this respect, we now perform an experiment using simulated data, to pin down the most important sources of the association between potential losses and frequency of trading. Specifically, we assess the impact of the sample size on potential losses, showing that as this increases, so do the potential losses. Further, we assess the impact of having heavy tails on the potential losses. We find that sample moments, when population moments are infinite, tend to be much higher than the SLLN would suggest, which we show is particularly true for the sample kurtosis.

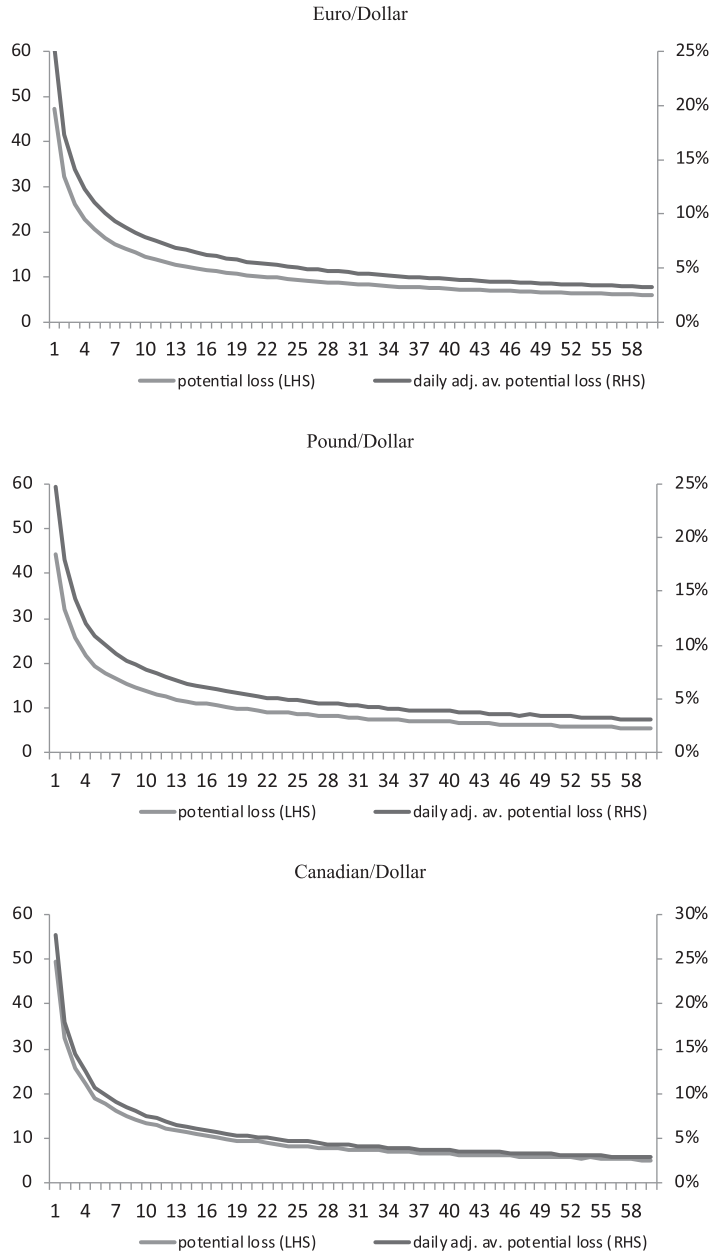

Fig 4. Trader's Potential Capital Losses, on the Three Futures Exchange Rates (Excluding Overnight Returns), above the Anticipated Losses from the *VaR* Measure.

NOTES: The *x*-axis denotes the m=1,...,60 minute intraday sampling (trading) frequencies. The values in the *y*-axis refer to number of times, whereas in the *z*-axis refers to percentages.

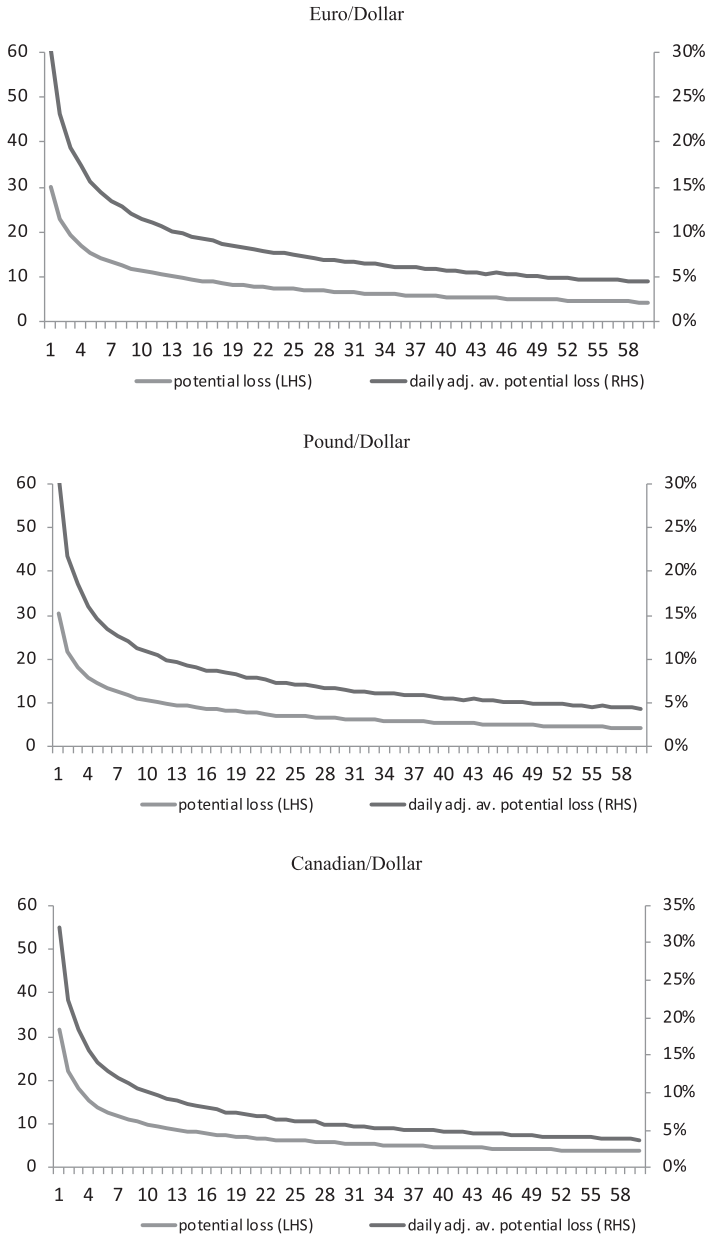

Fig 5. Trader's Potential Capital Losses, on the Three Futures Exchange Rates (Low Transaction Period), above the Anticipated Losses from the *VaR* Measure.

NOTES: The *x*-axis denotes the $m = 1,...,60$ minute intraday sampling (trading) frequencies. The values in the *y*-axis refer to number of times, whereas in the *z*-axis refers to percentages.

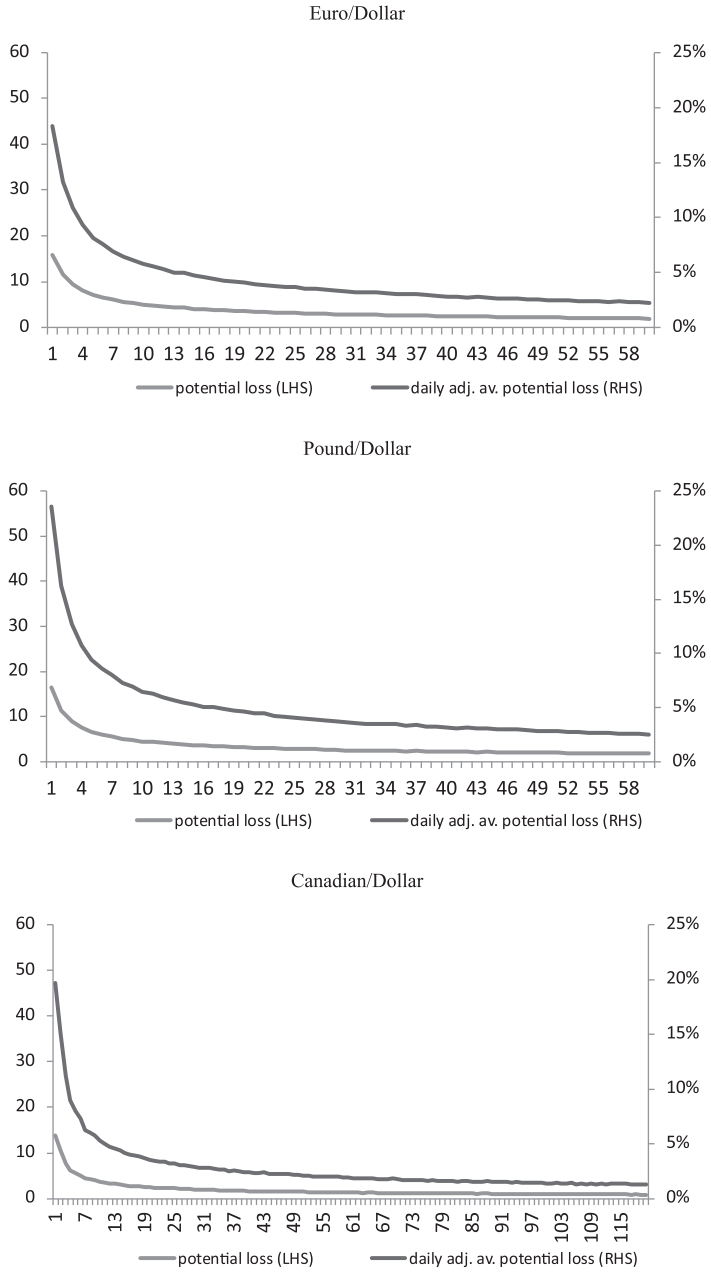

Fig 6. Trader's Potential Capital Losses, on the Three Futures Exchange Rates (High Transaction Period), above the Anticipated Losses from the *VaR* Measure.

NOTES: The *x*-axis denotes the m=1,...,60 minute intraday sampling (trading) frequencies. The values in the *y*-axis refer to number of times, whereas in the *z*-axis refer to percentages.

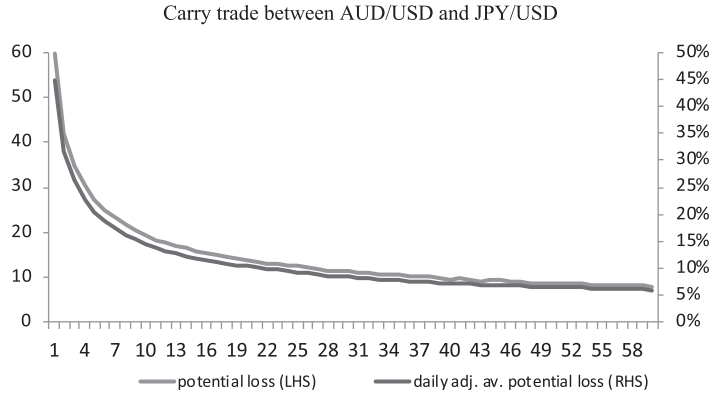

Fig 7. Trader's Potential Capital Losses, on the AUD/JPY Carry Trade, above the Anticipated Losses from the *VaR* Measure.

NOTES: The x-axis denotes the m=1,...,60 minute intraday sampling (trading) frequencies. The values in the y-axis refer to number of times, whereas in the z-axis refer to percentages.

3.1 Assessing the Impact of the Sample Size on Potential Losses

We analyze—via a simulation exercise—the impact of the sample size on potential losses, considering a Gaussian data generating process where we simulate the (log) prices, $\log(P_t)$, for $1 \leq t \leq 10^6$ as

$$\log(P_t) = \log(P_{t-1}) + z_t, \tag{12}$$

with $z_t \overset{i.i.d.}{\sim} N(0, 1/h^2)$, and initial price $P_1 = \$1,000$. The total sample is split in 1,000 trading days with 1,000 intraday prices. Without any loss of information, the sample $\{P_t\}_{t=1}^{10^6}$ mimics the P_{t_j} for $j = 1, \ldots, 1,000$ and $t = 1, \ldots, 1,000$, at sampling (or trading) frequency $m = 10^{-3}$. For example, at 1-minute sampling frequency, or $m = 10^{-3}$, we have $\tau = 1,000$ intraday prices, for $T = 1,000$ trading days, at 2-minutes sampling frequency, we have $\tau = 500$ intraday prices, for $T = 1,000$ trading days, and so on.

Figure 8 illustrates the $VaR^{(m)}_{(95\%)}$, the kurtosis of log-returns, $y_{t_j} = \log(P_{t_j}) - \log(P_{t-1_j})$, and the potential losses $L^{(m)}$, $\bar{L}^{(m)}$ for the simulated log-returns. We have set $h = 10$; we note, however, that, in unreported experiments, very similar results were found when using different values of h. The x-axis presents the trading frequency in minutes, from 1 up to 120 minutes. Without any loss of generality, we assume a long trading position; hence, the 95% *VaR* measure is computed as the 5% quantile point of the empirical distribution of y_{t_j}.[7]

7. For a short trading position, the 95% quantile point of the empirical distribution would have been considered.

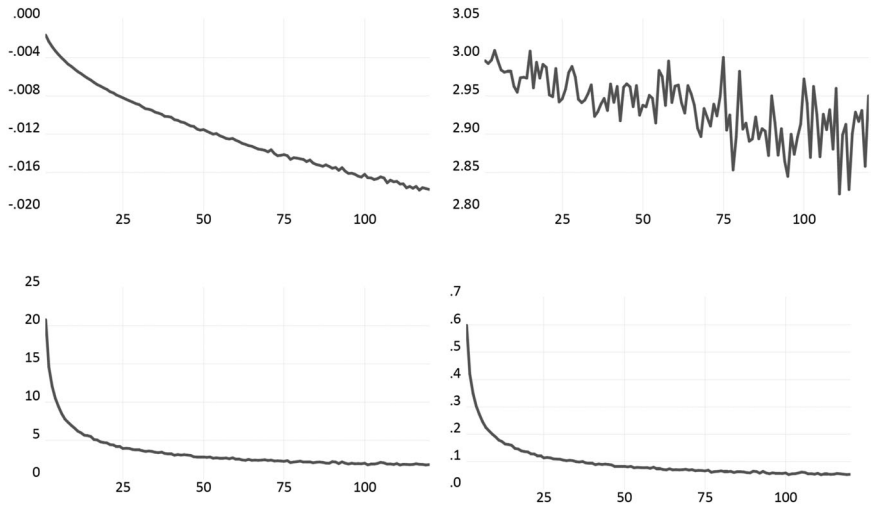

Fig 8. The Value-at-Risk, Kurtosis, and Potential Losses for the Random-Walk Data-Generated Process.

NOTES: The $VaR^{(m)}_{(95\%)}$ (upper left), the kurtosis of y_t (upper right), and the potential losses $L^{(m)}$ (lower left), $\bar{L}^{(m)}$ (lower right) for the simulated log-returns $y_{t_j} = \log(P_t/P_{t-1})$, for $\log(P_t) = \log(P_{t-1}) + z_t$, $z_t \overset{i.i.d.}{\sim} N(0, 1/h^2)$, $P_1 = \$1,000$ and $h = 10$. The x-axis denotes the $m = 1,...,120$ minute intraday sampling (trading) frequencies.

The simulated results provide us with an important finding: the potential losses are dependent on the trading frequency, where higher trading frequency leads to higher potential losses, despite the fact that the kurtosis (upper right graph) is around the value of 3 across any trading frequency $m = 1, \ldots, 120$. So, such finding could simply suggest that the increased potential losses are not related with the effect of *superkurtosis*, but rather they are the artifact output of the effect of number of observations that increases exponentially as the sampling frequency increases.

To shed further light on the impact of the sample size, we investigate the analytical form of the total potential losses. The potential loss $L^{(m)}$ is given by

$$L^{(m)} = \sum_{t=1}^{T} \sum_{j=1}^{\tau} \left(|y_{t_j} - VaR^{(m)}_{(1-p)}| \times I_{\{y_{t_j} < VaR^{(m)}_{(1-p)}\}} \right), \tag{13}$$

for $I_{\{.\}}$ representing the indicator variable and we compute the expected value of total potential losses, $\mathbb{E}(L^{(m)})$. For our long trading position and under the condition $y_{t_j} < VaR^{(m)}_{(1-p)}$, we have $y_{t_j} < 0$ and $VaR^{(m)}_{(1-p)} < 0$, as well. So, for $y_{t_j} < VaR^{(m)}_{(1-p)}$, we have $|y_{t_j} - VaR^{(m)}_{(1-p)}| = -(y_{t_j} - VaR^{(m)}_{(1-p)})$. Hence:

$$\mathbb{E}(L^{(m)}) = \sum_{t=1}^{T} \sum_{j=1}^{\tau} E\left(|y_{t_j} - VaR^{(m)}_{(1-p)}| \times I_{\{y_{t_j} < VaR^{(m)}_{(1-p)}\}} \right)$$

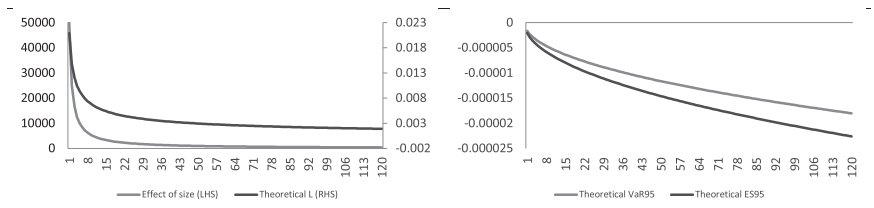

Fig 9. The Total Potential Losses, the Number of Observations ($T\tau$), the Expected Shortfall ($ES^{(m)}_{(1-p)}$), and the Value-at-Risk ($VaR^{(m)}_{(1-p)}$), under the Random-Walk Data-Generated Process, Per Sampling Frequency $m = 1, \ldots, 120$.

NOTES: The left panel shows the ($\mathbb{E}(L^{(m)})$) and the effect of size (i.e., number of observations, $T\tau$), per trading frequency $m = 1, \ldots, 120$, whereas the right panel shows the ES and the VaR, per trading frequency $m = 1, \ldots, 120$. The x-axis denotes the $m = 1$,...,120 minute intraday sampling (trading) frequencies.

$$= -\sum_{t=1}^{T}\sum_{j=1}^{\tau} p\mathbb{E}\Big(y_{t_j} - VaR^{(m)}_{(1-p)} | y_{t_j} < VaR^{(m)}_{(1-p)}\Big). \tag{14}$$

Note also that $\mathbb{E}(I_{\{y_{t_j} < VaR^{(m)}_{(1-p)}\}}) = p$, as well as, that $\mathbb{E}(y_{t_j} | y_{t_j} < VaR^{(m)}_{(1-p)}) = ES^{(m)}_{(1-p)}$, and that $\mathbb{E}(VaR^{(m)}_{(1-p)} | y_{t_j} < VaR^{(m)}_{(1-p)}) = VaR^{(m)}_{(1-p)}$. Hence, it follows that

$$\mathbb{E}(L^{(m)}) = -T\tau p(ES^{(m)}_{(1-p)} - VaR^{(m)}_{(1-p)}). \tag{15}$$

Under the data-generated process of equation (12), it is easy to see that,

$$VaR^{(m)}_{(1-p)} = \Phi_{(1-p)}\left(\mathbb{E}(y_{t_j}) = 0, V(y_t) = \left(\sqrt{\frac{m}{h^2}}\right)^2\right) \tag{16}$$

and

$$ES^{(m)}_{(1-p)} = -\frac{\sigma}{1-p}\varphi\big(\Phi_{(1-p)}(0,1)\big), \tag{17}$$

where $\varphi(\cdot)$ denotes the standard normal probability density function and $\sigma = h^{-1}\sqrt{m}$. Hence, the $VaR^{(m)}_{(1-p)}$ measure equals to the $(1-p)$ percentile point of the inverse cumulative normal distribution with zero mean and $h^{-1}\sqrt{m}$ standard deviation (we would like to bring to the reader's attention that $m = \tau^{-1}$ is the intraday trading frequency).

So, as presented in Figure 9, the total potential losses per trading frequency m are not only affected by the number of observations ($T\tau$, which denotes the effect of size), but also from the distance between the two risk measures; that is, the expected shortfall and the VaR, that is, $(ES^{(m)}_{(1-p)} - VaR^{(m)}_{(1-p)})$. Therefore, as the trading frequency increases, *(i)* the number of trades increases exponentially (see the effect of size in Figure 9), while *(ii)* the distance between the two risk measures decreases (see the

expected shortfall and value-at-risk in Figure 9). Indicatively, some estimates of (15) are $\mathbb{E}(L^{(1)}) = 0.02089$ and $\mathbb{E}(L^{(120)}) = 0.00191$, for $ES^{(1)}_{(5\%)} - VaR^{(1)}_{(5\%)} = 4.2E-7$ and $ES^{(120)}_{(5\%)} - VaR^{(120)}_{(5\%)} = 4.6E-6$.

Thus, both analytical and simulated evidences show that the total potential losses per trading frequency m are affected positively by the number of trades and negatively by the distance between the two risk measures. Having established the aforementioned effects, in the paragraphs that follow, we investigate whether there are any additional effects from the infinity of moments.

Assessing the impact of heavy tails on potential losses. We now turn to investigating the effect of heavy tails on potential losses; in particular, we assess the impact of *superkurtosis*. To this end, we consider a heavy tailed data-generating process, as follows:

$$\log(P_t) = \log(P_{t-1}) + z_t, \tag{18}$$

for $z_t \overset{i.i.d.}{\sim} t(0, 1/h^2, v)$, for $v \geq 2$ and initial price of $P_1 = \$1,000$. The probability density function for Student t is considered as: $\varphi(0, 1/h^2, v) = \frac{\Gamma(\frac{v+1}{2})}{\Gamma(\frac{v}{2})\sqrt{\frac{\pi v}{h^2}}}(1 + \frac{z_t^2 h^2}{v})^{-\frac{v+1}{2}}$.

Figure 10 shows the values of the sample kurtosis and the potential losses $L^{(m)}$, $\bar{L}^{(m)}$ for the simulated log-returns, from the Student t random-walk data-generated process under various degrees of freedom, $v = 3, 4, 5, 10, 30, 100$ and $h = 10$; clearly, the population kurtosis does not exist for the first two values.

We note that, for the near-Gaussian cases $v = 30$ and 100, the kurtosis remains constant across various values of trading frequency, and, as expected, the potential losses $L^{(m)}$ and $\bar{L}^{(m)}$ are almost identical to those found in the previous section. As is natural to expect, as the degree of freedom v decreases, the sample kurtosis increases; for example, for $v = 10$, the kurtosis of log-returns at 120-minutes trading frequency is around 3.1, whereas for $v = 3$, the kurtosis of log-returns at 120-minutes trading frequency is around 3.6. However, Figure 10 shows a remarkable feature of the sample kurtosis. Heuristically, when $v \leq 4$, the sample kurtosis should pass to infinity as the sample size $T\tau \to \infty$; in particular, the Marcinkiewicz–Zygmund SLLN implies that the sample kurtosis should pass to infinity at a rate given by (modulo some slowly varying sequence) $O((T\tau)^{\frac{4-v}{v}})$. For example, when $v = 3$, the sample kurtosis should diverge to infinity as fast as (approximately) $O((T\tau)^{1/3})$. Based on these heuristic considerations, when, for example, $v = 3$, one could expect the sample kurtosis for the 1-minute trading frequency to be larger by a factor $120^{1/3}$ than the sample kurtosis calculated for the 120-minutes trading frequency, keeping T constant. On the contrary, from Figure 10, it is apparent that the sample kurtosis is larger than the theory would predict. For example, for $v = 3$, the 1-minute sampling frequency log-returns have kurtosis of 96, which is approximately 26 times as much as in the 120-minute sampling frequency case, whereas the theory would predict an increase of approximately five times only.

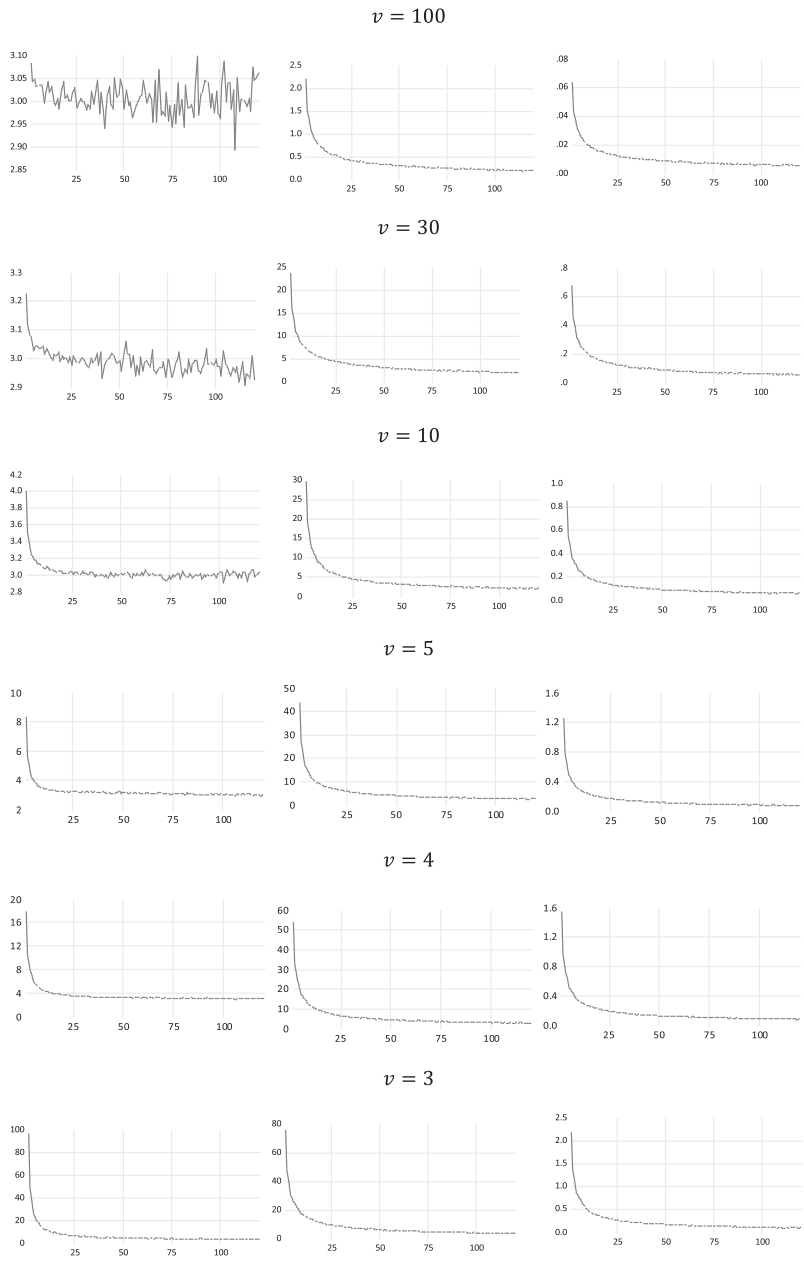

Fig 10. The Total Potential Losses and Kurtosis from the Student t Random-Walk Data-Generated Process under Various Degrees of Freedom.

NOTES: The kurtosis of y_t (left panel), the potential losses $L^{(m)}$ (middle panel), and the $\bar{L}^{(m)}$ (right panel) from the Student t random-walk data-generated process under various degrees of freedom, v, $\log(P_t) = \log(P_{t-1}) + z_t$, $z_t \overset{i.i.d.}{\sim} t(0, 1/h^2, v)$, $P_1 = \$1,000$, $h = 10$. The x-axis denotes the $m = 1,...,120$ minute intraday (trading) sampling frequencies.

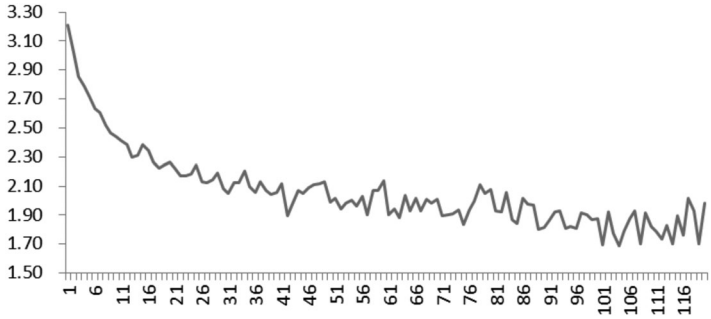

Fig 11. The Effect of Superkurtosis on Potential Losses across Different Sampling Frequencies.

NOTES: The figure presents the ratio of the potential losses ($L^{(m)}$) from the Student t random-walk data-generated process under 3 and 30 degrees of freedom. The x-axis denotes the $m = 1,...,120$ minute intraday (trading) sampling frequencies.

Turning now to the relationship between kurtosis and potential losses at the highest trading frequency of 1 minute, we document that a kurtosis of 4 (as derived for $v = 10$ degrees of freedom) implies potential losses of $L^{(1)} = 27.8$ and $\bar{L}^{(1)} = 0.80$, whereas a kurtosis of 96 (as derived for $v = 3$) increases the potential losses to $L^{(1)} = 75.8$ and $\bar{L}^{(1)} = 2.18$.

To segregate the effect of the mechanically increasing sample size from this of the *superkurtosis*, we normalize the potential loss measure so to remove the effect of the former. To do so, we compute the ratio of the potential losses across sampling frequencies from the data-generated process $\log(P_t) = \log(P_{t-1}) + z_t$, for $z_t \overset{i.i.d.}{\sim} t(0, 1/h^2, v)$, at different degrees of freedom. Indicatively, Figure 11 presents the ratio of potential losses for $v = 3$ and $v = 30$ degrees of freedom. For example, at 1-minute sampling frequency the $L^{(1)}$ for $v = 3$ is 75.43 and for $v = 30$ is 23.49; hence the ratio, as presented in Figure 11, is 3.21 times. In other words, *superkurtosis* leads to 3.3 times higher potential losses at 1-minute sampling frequency. This finding holds across all sampling frequencies; however, it is evident that as the sampling frequency increases, the effect of *superkurtosis* is magnified exponentially.

Both simulated and analytical results strengthen our findings, from the real data, that the potential losses are dependent on the trading frequency, where higher trading frequency leads to higher potential losses. Most importantly, though, we observe the effect of *superkurtosis*, which is also evident in the real data, to influence radically the potential losses. Put differently, the shape of the potential losses from the simulated data does resemble those of the actual data. Thus, as the sampling (trading) frequency increases, the effect of *superkurtosis* becomes more material and the potential losses increase substantially.

Finally, we would like to highlight that we have further experimented with the previous simulation for $P_1 = 1$ in order to mimic the exchange rate values, as well as, using a conditionally heteroskedastic data-generating process and the results remain robust.[8]

8. Results are not reported in this paper for the sake of brevity, and they are available upon request.

4. DISCUSSION AND CONCLUSIONS

It is common practice for risk metrics users to assume that the moments of asset returns are finite, and to use this assumption to capture the potential losses from asset trading, using metrics such as the *VaR* or *ES*. While this assumption appears to be correct for daily frequencies, it is not clear whether this also entails that it holds for higher, intraday frequencies. Further, if this assumption fails to hold, it is not clear what the likely consequences are. On the other hand, while computing the *VaR* under non-Gaussian assumptions is perfectly possible, existing methodologies require several assumptions that, if not satisfied, may make calculations unreliable. Hence, it is important to have a methodology to verify whether the assumption of finite higher order moments is adequate.

In this paper, we make two contributions. First, we develop a (replicable) methodology to assess whether the moments of intraday data are finite or not. Second, we thoroughly assess the potential losses arising from intraday trading, when a risk management metric, such as *VaR* or *ES*, is used under the implicit assumption that the higher order moments of asset returns are finite. Using both real data and a simulation exercise, we (unsurprisingly) find that, when daily trading is implemented, *VaR* estimates work as expected, with potential losses being in line with what the theory predicts. Conversely, results are far from standard when high-frequency, intraday trading is considered. In this case, the potential losses are much larger than what the theory predicts. We show that there are two concurring features that can explain our findings. First, the sample size itself: as the sampling frequency increases, so does the number of datapoints; hence, our results show that this (obviously) increases the potential losses. Second and more importantly, intraday data are more likely to have heavy tails. In our simulations, we show that the sample kurtosis computed using data sets with infinite fourth moment tends to be much higher than what the theory would predict, which, in turn, further increases the potential losses. We call this discrepancy between the theoretical behavior and the actual magnitude of the sample kurtosis *superkurtosis*, and we argue that it is one component of the heavy potential losses that, as a stylized fact, are encountered when trading at intraday frequency under the (implicit in the use of *VaR* or *ES*) assumption that high-order moments are finite when, in fact, they are infinite.

Our findings entail that employing traditional risk measures for market participants who engage in intraday trading imposes serious threats to the stability of financial markets, given that capital ratios may be severely underestimated. Indeed, based on our analysis, it follows that the hidden risks from intraday trading in the foreign exchange market alone in the financial system are immense, and minimum capital requirement must be substantially increased in such higher trading frequencies, so that risk metrics like *VaR* or *ES* match the central bank's capital adequacy preset levels for financial stability reasons.

Currently, the importance of the frequency of trading is typically underplayed. For instance, the Fundamental Review of the Trading Book framework recently finalized by the ECB[9] emphasizes the importance of including risk factors such as the *ES* in an institution's risk metrics, but it does not offer any guidance as to how a risk factor might change in value when trading takes place at extremely high frequency or how the fair value of a trading asset might be impacted by the frequency of trading. Perhaps more importantly, our findings also have implications for the development of the financial institutions risk assessments metrics set by the Bank for International Settlements (BIS). Appropriate risk measurement is key to the assessment of both firm-specific risk and of aggregate risk, independently of the leverage used by financial institutions. In this sense, if capital requirements, which are designed to mitigate the losses incurred in extreme events, are mismeasured, then they do not solve the underlying problem that arises from a potential underestimation of actual risks that arise from intraday trading. For instance, in the most recent report of BIS for the minimum capital requirements for market risk, in 2019,[10] the severity of intraday trading is acknowledged, noting that banks "are expected to maintain strict risk management systems to ensure that intraday exposures are not excessive" (p. 13)—yet maintaining the suggestion that risk metrics, such as *ES*, should be computed on a daily basis.

The main purpose of this paper is to highlight the stylized fact that intraday trading is based on data with infinite high-order moments, and that this invalidates the standard *VaR* and *ES* metrics. However, our results also have clear policy implications. Indeed, an immediate conclusion from our findings is that central banks, and banking supervisory authorities, should make use of more appropriate risk metrics that reflect the presence of *superkurtosis*. Several alternatives could be proposed to the classical *VaR*. For example, a naive, but arguably robust, methodology could be based on multiplying the standard, "Gaussian" estimate of a risk metric by a factor K to take account of the increased trading frequency and of its impact of superkurtosis. Such a factor could be calibrated, for example, by simulation, based on the sample moments of the data at hand. An alternative, more classical, approach could be based on choosing a flexible family of distributions (e.g., the generalized Pareto distribution), and using the quantiles thereof instead of the quantiles of the Gaussian distribution. The choice of an appropriate parametric form, in such a case, would be of pivotal importance, as well as the development of a robust estimator. Having a correct measurement of risk metrics is bound to enhance the effectiveness of the macroprudential policies (such as the countercyclical capital buffers and minimum capital requirements), by reducing the vulnerabilities of the financial system, and thus, leading to higher financial stability.

Now more than ever, the use of the correct high-frequency risk metrics is of paramount importance, given the ultrafast emergence of new assets that reflect no

9. https://www.eba.europa.eu/regulation-and-policy/market-risk/draft-technical-standards-on-the-ima-under-the-frtb

10. https://www.bis.org/bcbs/publl/d457.pdf

economic fundamentals but are heavily traded by market participants, like cryptocurrency perpetual futures, imposing real risks at the very heart of the financial system. The important issues mentioned above are under investigation by the authors.

ACKNOWLEDGMENTS

We are very grateful to the Editor (Pok-sang Lam) and to an anonymous Referee for providing many valuable comments that have greatly improved the quality and generality of our paper. We would also like to thank Rafael La Porta, Adam McCloskey, Lucio Sarno, and Ron Smith for their valuable comments.

LITERATURE CITED

Beddington, John, Clara Furse, Philip Bond, Dave Cliff, Charles Goodhart, Kevin Houstoun, Oliver Linton, and Jean-Pierre Zigrand. (2012) "Foresight: The Future of Computer Trading in Financial Markets: Final Project Report."

Bradley, Brendan O., and Murad S. Taqqu. (2003) "Financial Risk and Heavy Tails." In *Handbook of Heavy Tailed Distributions in Finance*, edited by Svetlozar T. Rachev, pp. 35–103. Amsterdam: North-Holland.

Brush, Silla, T. Schoenberg, and Suzi Ring. (2015) "How A Mystery Trader with an Algorithm May Have Caused the Flash Crash."*Bloomberg News*, 22.

Geyer, Charles J., and Glen D. Meeden. (2005) "Fuzzy and Randomized Confidence Intervals and P-Values." *Statistical Science*, 20, 358–66.

Horváth, Lajos, and Lorenzo Trapani. (2019) "Testing for Randomness in a Random Coefficient Autoregression Model. " *Journal of Econometrics*, 209, 338–52.

Kirilenko, Andrei, Albert S. Kyle, Mehrdad Samadi, and Tugkan Tuzun. (2017) "The Flash Crash: High-Frequency Trading in an Electronic Market. " *Journal of Finance*, 72, 967–98.

Kirilenko, Andrei A., and Andrew W. Lo. (2013) "Moore's Law versus Murphy's Law: Algorithmic Trading and its Discontents. " *Journal of Economic Perspectives*, 27, 51–72.

Manganelli, Simone, and Robert F. Engle. (2001) "Value at Risk Models in Finance." Technical Report.

Manhire, Jack T. (2018) "Measuring Black Swans in Financial Markets." *Journal of Mathematical Finance*, 8, 227–39.

Michel, Reinhard. (1976) "Nonuniform Central Limit Bounds with Applications to Probabilities of Deviations." *Annals of Probability*, 4, 102–6.

Trapani, Lorenzo. (2016) "Testing for (in) Finite Moments. " *Journal of Econometrics*, 191, 57–68.

Yadav, Yesha. (2015) "How Algorithmic Trading Undermines Efficiency in Capital Markets. " *Vanderbilt Law Review*, 68, 1607.

APPENDIX A: COMPLEMENTS TO SECTION 1

We report some results that are referred to in the main paper, and the proof of Theorem 2.

A.1 Construction of μ_k. In the construction of μ_k, we begin by noting that we apply the tests to demeaned data.

The first statistic to be employed is μ_2, which has been designed to test for $H_0 : E|X|^2 = \infty$—that is, the nonexistence of the variance. When $k = 2$, the sample second moment (at the numerator) is made scale-invariant by dividing by the square of the mean absolute value of x_t; other rescalings would be possible (chiefly, the median, which has the advantage of being well defined), but the simulations in Trapani (2016) show that the mean absolute value yields better power and size.

For $k = 3, 4$, rescaling is done using the sample variance, as is more natural. The rationale for these choices is also discussed in Trapani (2016). Here, we point out that we need a scale invariant test statistic, that is, a sample moment that is not sensitive to the unit of measurement of the data. The sample variance is an obvious candidate for this, as a "natural" measure of scale. The simulations in Trapani (2016) also show that it works well in finite samples. In general, other rescalings could be considered, based on a sample moment of order lower than k. As mentioned also in Section 1, letting $p < k$, one could compute

$$\mu_p = \frac{1}{T}\sum_{t=1}^{T} |x_t|^p, \tag{A.1}$$

and then define the statistic

$$\widetilde{\mu}_k = \frac{T^{-1}\sum_{t=1}^{T} |x_t|^k}{\mu_p^{k/p}}. \tag{A.2}$$

Trapani (2016) shows that Theorem 1 holds for all $p < k$ (see in particular Section 3.1 in that paper).

Finally, we note that, in the formula that defines μ_k, some constants are used, denoted as c_k. These are taken directly from Trapani (2016), where they are defined as

$$c_k = \begin{cases} \frac{4}{\pi} & \text{when } k = 2 \\ 1 & \text{when } k = 3 \\ l\frac{1}{3} & \text{when } k = 4 \end{cases}. \tag{A.3}$$

The rationale underpinning the choice of c_k is as follows. The test works by evaluating whether a sample moment is "very large" (so that the corresponding population moment is infinite) or "sufficiently small" (which, conversely, implies that the population moment is finite). As mentioned above, the notions of being large or small are only relative notions, that is, relative to a benchmark: Trapani (2016) argues that,

letting $Z \sim N(0, 1)$, a useful term of comparison for the sample kth-order moment of the data could be $c_k = E|Z|^k$.

A.2 Asymptotic Behavior of $\Theta^{(k)}_{T,R}$. Let "$\xrightarrow{d^*}$" and "$\xrightarrow{P^*}$" denote convergence in distribution and in probability, respectively, with respect to the probability conditional on the sample $\{x_t\}_{t=1}^T$, say P^*. We summarize the properties of the test above in the following theorem.[11]

THEOREM 1. *We assume that the assumptions of Theorem 1 in Trapani (2016) are satisfied, and that* $R = O(T)$. *Then, as* $\min(T, R) \to \infty$, *it holds that*

$$\Theta^{(k)}_{T,R} \xrightarrow{d^*} \chi^2_1, \text{ under } H_0, \tag{A.4}$$

$$R^{-1}\Theta^{(k)}_{T,R} \xrightarrow{P^*} 1, \text{ under } H_A, \tag{A.5}$$

for almost all realizations of $\{x_t\}_{t=1}^T$.

We now present a result on the behavior of $Q^{(k)}(\alpha)$.

THEOREM 2. *We assume that the assumptions of Theorem 1 are satisfied, and that* $S = c_0 R$ *for some* $0 < c_0 < \infty$. *Then, as* $\min(T, R) \to \infty$, *it holds that there exist a triple of random variables* T_0, R_0, S_0 *such that, for* $T \geq T_0$, $R \geq R_0$, *and* $S \geq S_0$

$$Q^{(k)}(\alpha) \geq (1 - \alpha) - \sqrt{\alpha(1 - \alpha)}\sqrt{\frac{2 \log\log S}{S}}, \tag{A.6}$$

under H_0, *and*

$$Q^{(k)}(\alpha) \leq \epsilon, \tag{A.7}$$

under H_A, *for almost all realizations of* $\{x_t, 1 \leq t \leq T\}$ *and all* $\epsilon > 0$.

PROOF. We begin by noting that $E^*I[\Theta^{(k)}_{T,R,s} \leq c_\alpha] = P^*(\Theta^{(k)}_{T,R,s} \leq c_\alpha)$. From the proof of Theorem 1 in Trapani (2016) (see also more explicit calculations in Horváth and Trapani 2019), we know that

$$\Theta^{(k)}_{T,R,s} = X_{R,s} + Y_{R,s}, \tag{A.8}$$

where

$$X_{R,s} = \left(2R^{-1/2}\sum_{j=1}^{R}\left(\zeta^{(k)}_{j,T,s}(0) - \frac{1}{2}\right)\right)^2, \tag{A.9}$$

11. The proof can be derived using exactly the same arguments as in Horváth and Trapani (2019), and we do not report it here to save space.

and Horváth and Trapani (2019) show that the remainder $Y_{R,s}$ is such that $E^*Y_{R,s}^2 = c_0(\psi_k^{-1} + R\psi_k^{-2})$—henceforth, we omit the dependence on s when possible. Let now $\epsilon_T = (\psi_k^{-1} + R\psi_k^{-2})^{1/3}$, and note that, using elementary arguments

$$P^*\left(\Theta_{T,R,s}^{(k)} \leq c_\alpha\right) \leq P^*(X_R \leq c_\alpha + \epsilon_T) + P^*(|Y_R| \geq \epsilon_T). \tag{A.10}$$

Thus,

$$P^*\left(\Theta_{T,R,s}^{(k)} \leq c_\alpha\right) - P^*(X_R \leq c_\alpha) \tag{A.11}$$

$$\leq P^*(X_R \leq c_\alpha + \epsilon_T) - P^*(X_R \leq c_\alpha) + P^*(|Y_R| \geq \epsilon_T). \tag{A.12}$$

Markov inequality immediately yields $P^*(|Y_R| \geq \epsilon_T) \leq \epsilon_T^{-2} E^* Y_R^2 = c_0(\psi_k^{-1} + R\psi_k^{-2})^{1/3}$. Also note that

$$P^*(X_R \leq c_\alpha + \epsilon_T) - P^*(X_R \leq c_\alpha) \tag{A.13}$$

$$\begin{aligned} &= P^*(X_R \leq c_\alpha + \epsilon_T) \pm P\big(Z^2 \leq c_\alpha + \epsilon_T\big) \\ &- \big[P^*(X_R \leq c_\alpha) \pm P\big(Z^2 \leq c_\alpha\big)\big], \end{aligned} \tag{A.14}$$

where $Z \sim N(0, 1)$. Using Taylor's expansion, it is easy to see that

$$P\big(Z^2 \leq c_\alpha + \epsilon_T\big) - P\big(Z^2 \leq c_\alpha\big) \leq c_0 \epsilon_T. \tag{A.15}$$

Also, by the Berry–Esseen theorem (see, e.g., Michel 1976), it holds that

$$\left|P^*(X_R \leq c_\alpha + \epsilon_T) - P\big(Z^2 \leq c_\alpha + \epsilon_T\big)\right| \leq c_0 \frac{R^{-1/2}}{1 + |c_\alpha + \epsilon_T|^{3+\delta}}, \tag{A.16}$$

for all $\delta \geq 0$. Finally, using again the Berry–Esseen theorem,

$$\left|P^*(X_R \leq c_\alpha) - P\big(Z^2 \leq c_\alpha\big)\right| \leq c_0 \frac{R^{-1/2}}{1 + |c_\alpha|^{3+\delta}}. \tag{A.17}$$

Putting all together, it follows that

$$\left|P^*\left(\Theta_{T,R,s}^{(k)} \leq c_\alpha\right) - P\big(Z^2 \leq c_\alpha\big)\right| \leq c_0\big(R^{-1/2} + \epsilon_T\big). \tag{A.18}$$

Hence, we have

$$\sqrt{\frac{S}{2\log\log S}} \frac{Q^{(k)}(\alpha) - (1-\alpha)}{\sqrt{\alpha(1-\alpha)}} = \sqrt{\frac{S}{2\log\log S}} \frac{S^{-1}\sum_{s=1}^{S} Z_s - (1-\alpha)}{\sqrt{\alpha(1-\alpha)}}$$

$$+c_0\sqrt{\frac{S}{2\log\log S}}\left(R^{-1/2}+\epsilon_T\right), \quad \text{(A.19)}$$

where $\{Z_s, 1 \le s \le S\}$ is an *i.i.d.* sequence with common distribution $Z_1 \sim N(0,1)$. By Trapani (2016), it follows that

$$\sqrt{\frac{S}{2\log\log S}}\left(R^{-1/2}+\epsilon_T\right) = o_{a.s.}(1); \quad \text{(A.20)}$$

the desired result now follows from the law of the iterated logarithm. □

APPENDIX B: DESCRIPTIVE STATISTICS

TABLE B.1

DESCRIPTIVE STATISTICS OF THE THREE CURRENCY PAIRS AT DIFFERENT SAMPLING (TRADING) FREQUENCIES

Frequency	*Mean*	*Std.Dev.*	*Skewness*	*Kurtosis*	*Mean*	*Std.Dev.*	*Skewness*	*Kurtosis*
	EUR/USD futures				*EUR/USD spot*			
1 m	1.34×10^{-8}	1.88×10^{-4}	1.806	729.97	8.29×10^{-8}	1.80×10^{-4}	0.337	79.58
2 m	2.68×10^{-8}	2.63×10^{-4}	1.396	395.10	1.66×10^{-7}	2.55×10^{-4}	0.117	71.02
5 m	6.70×10^{-8}	4.07×10^{-4}	0.799	161.38	4.14×10^{-7}	3.97×10^{-4}	0.155	45.01
10 m	1.34×10^{-7}	5.69×10^{-4}	0.545	85.43	8.29×10^{-7}	5.55×10^{-4}	0.071	26.34
15 m	2.01×10^{-7}	6.92×10^{-4}	0.439	62.34	1.24×10^{-6}	6.78×10^{-4}	0.353	30.59
20 m	2.68×10^{-7}	7.94×10^{-4}	0.469	52.64	1.66×10^{-6}	7.78×10^{-4}	−0.001	20.03
30 m	4.01×10^{-7}	9.70×10^{-4}	0.304	36.85	2.49×10^{-6}	9.51×10^{-4}	0.173	20.65
60 m	8.02×10^{-7}	13.28×10^{-4}	0.271	24.67	4.97×10^{-6}	13.35×10^{-4}	0.047	13.93
Daily	8.99×10^{-5}	64.48×10^{-4}	0.033	4.33	5.93×10^{-6}	63.12×10^{-4}	0.198	6.55
	GBP/USD futures				*GBP/USD spot*			
1 m	-6.52×10^{-9}	1.78×10^{-4}	−0.487	269.39	-7.92×10^{-9}	1.74×10^{-4}	−0.025	46.44
2 m	-1.30×10^{-8}	2.12×10^{-4}	−0.500	119.22	-1.59×10^{-8}	2.47×10^{-4}	−0.088	48.42
5 m	-3.25×10^{-8}	3.16×10^{-4}	−0.422	85.45	-3.99×10^{-8}	3.86×10^{-4}	−0.096	32.66
10 m	-6.49×10^{-8}	4.42×10^{-4}	−0.364	61.41	-8.17×10^{-8}	5.41×10^{-4}	−0.107	25.23
15 m	-9.76×10^{-8}	5.29×10^{-4}	−0.348	36.53	-1.23×10^{-7}	6.55×10^{-4}	−0.075	21.23
20 m	-1.30×10^{-7}	6.16×10^{-4}	−0.345	41.92	-1.67×10^{-7}	7.57×10^{-4}	−0.129	24.21
30 m	-1.95×10^{-7}	7.44×10^{-4}	−0.317	27.83	-2.45×10^{-7}	9.18×10^{-4}	−0.056	17.84
60 m	-3.93×10^{-7}	10.14×10^{-4}	−0.288	19.71	-4.94×10^{-7}	12.91×10^{-4}	−0.113	16.15
Daily	6.22×10^{-5}	56.79×10^{-4}	−0.321	5.33	-5.96×10^{-6}	60.99×10^{-4}	0.357	8.12
	CAD/USD futures				*CAD/USD spot*			
1 m	1.63×10^{-8}	1.87×10^{-4}	0.116	103.30	1.74×10^{-8}	1.97×10^{-4}	0.049	40.32
2 m	3.25×10^{-8}	2.57×10^{-4}	0.067	64.32	3.48×10^{-8}	2.77×10^{-4}	−0.045	40.25
5 m	8.14×10^{-8}	3.96×10^{-4}	0.029	39.46	8.59×10^{-8}	4.32×10^{-4}	−0.033	24.17
10 m	1.63×10^{-7}	5.51×10^{-4}	0.049	29.89	1.73×10^{-7}	6.00×10^{-4}	−0.079	19.89
15 m	2.44×10^{-7}	6.64×10^{-4}	−0.035	24.33	2.59×10^{-7}	7.34×10^{-4}	−0.002	18.88
20 m	3.25×10^{-7}	7.63×10^{-4}	0.067	22.01	3.45×10^{-7}	8.41×10^{-4}	−0.038	16.45
30 m	4.87×10^{-7}	9.24×10^{-4}	0.021	19.25	5.18×10^{-7}	10.26×10^{-4}	0.067	15.13
60 m	9.71×10^{-7}	12.31×10^{-4}	0.192	17.48	1.03×10^{-6}	14.35×10^{-4}	0.044	14.50
Daily	5.09×10^{-5}	58.10×10^{-4}	−0.142	6.01	1.50×10^{-5}	65.76×10^{-4}	0.002	6.40